Inorg. Chem. **2004**, *43*, 3106–3115

Proton Transfer to Nickel–Thiolate Complexes. 2. Rate-Limiting Intramolecular Proton Transfer in the Reactions of $[Ni(SC_6H_4R\text{-}4)(PhP\{CH_2CH_2PPh_2\}_2)]^+$ (R = NO_2, Cl, H, Me, or MeO)

Valerie Autissier,[†] Pedro Martin Zarza,[‡] Athinoula Petrou,[§] Richard A. Henderson,*[,†] Ross W. Harrington,[†] and William C. Clegg[†]

Department of Chemistry, School of Natural Sciences, University of Newcastle, Newcastle upon Tyne, NE1 7RU U.K., Departamento de Química Inorgánica, Universidad de La Laguna, 38200 La Laguna, Tenerife, Spain, and Laboratory of Inorganic Chemistry, University of Athens, Panepistimioupolis, Athens, 15771 Greece

Received November 14, 2003

The protonation of $[Ni(SC_6H_4R\text{-}4)(triphos)]^+$ (triphos = $PhP\{CH_2CH_2PPh_2\}_2$; R = NO_2, Cl, H, Me, or MeO) by $[lutH]^+$ (lut = 2,6-dimethylpyridine) to form $[Ni(S(H)C_6H_4R\text{-}4)(triphos)]^{2+}$ is an equilibrium reaction in MeCN. Kinetic studies, using stopped-flow spectrophotometry, reveal that the reactions occur by a two-step mechanism. Initially, $[lutH]^+$ rapidly binds to the complex (K_2^R) in an interaction which probably involves hydrogen-bonding of the acid to the sulfur. Subsequent intramolecular proton transfer from $[lutH]^+$ to sulfur (k_3^R) is slow because of both electronic and steric factors. The X-ray crystal structures of $[Ni(SC_6H_4R\text{-}4)(triphos)]^+$ (R = NO_2, H, Me, or MeO) show that all are best described as square-planar complexes, with the phenyl substituents of the triphos ligand presenting an appreciable barrier to the approach of the sterically demanding $[lutH]^+$ to the sulfur. The kinetic characteristics of the intramolecular proton transfer from $[lutH]^+$ to sulfur have been investigated. The rate of intramolecular proton transfer exhibits a nonlinear dependence on Hammett σ^+, with both electron-releasing and electron-withdrawing 4-R-substituents on the coordinated thiolate facilitating the rate of proton transfer (NO_2 > Cl > H > Me < MeO). The rate constants for intramolecular proton transfer correlate well with the calculated electron dnsity of the sulfur. The temperature dependence of the rate of the intramolecular proton transfer reactions shows that $\Delta H^‡$ is small but increases as the 4-R-substituent becomes more electron-withdrawing {$\Delta H^‡$ = 4.1 (MeO), 6.9 (Me), 11.4 kcal mol^{-1} (NO_2)}, while $\Delta S^‡$ becomes progressively less negative {$\Delta S^‡$ = –50.1 (MeO), –41.2 (Me), –16.4 (NO_2) cal K^{-1} mol^{-1}}. Studies with $[lutD]^+$ show that the rate of intramolecular proton transfer varies with the 4-R-substituent {$(k_3^{NO_2})^H/(k_3^{NO_2})^D$ = 0.39; $(k_3^{Cl})^H/(k_3^{Cl})^D$ = 0.88; $(k_3^{Me})^H/(k_3^{Me})^D$ = 1.3; $(k_3^{MeO})^H/(k_3^{MeO})^D$ = 1.2}.

Introduction

In the previous paper[1] we described mechanistic studies on the equilibrium proton transfer reactions of $[Ni(SC_6H_4R\text{-}4)_2(dppe)]$ (R = MeO, Me, H, Cl, or NO_2; dppe = $Ph_2PCH_2CH_2PPh_2$) with mixtures of $[lutH]^+$ and lut (lut = 2,6-dimethylpyridine). We showed that the reactions were characterized by the following features. (i) Proton transfer rates are slow. (ii) The pK_a's of the corresponding $[Ni(SHC_6H_4R\text{-}4)(SC_6H_4R\text{-}4)(dppe)]^+$ are only slightly affected by the 4-R-substituent. (iii) The rates of proton transfer show a marked nonlinear dependence on the nature of the 4-R-substituent, with both electron-withdrawing and electron-releasing substituents facilitating proton transfer. (iv) The values of $\Delta H^‡$ and $\Delta S^‡$ for proton transfer[2] show a marked dependence on the nature of the 4-R-substituent, consistent with a transition state for proton transfer in which the extent of proton transfer is affected by the 4-R-substituent. (v) With $[Ni(SC_6H_4NO_2\text{-}4)_2(dppe)]$ the kinetics indicate a two-step process in which initial hydrogen-bond formation between

* To whom correspondence should be addressed. E-mail: r.a.henderson@ncl.ac.uk.
[†] University of Newcastle.
[‡] Universidad de La Laguna.
[§] University of Athens.

(1) Accompanying paper: Autissier, V. A.; Clegg, W.; Harrington, R. W.; Henderson, R. A. *Inorg. Chem.* **2004**, *43*, 3098−3105.
(2) (a) Marcus, R. A. *J. Am. Chem. Soc.* **1969**, *91*, 7224. (b) Albery, W. J. *Faraday Discuss. Chem. Soc.* **1982**, *74*, 245.

10.1021/ic0303237 CCC: $27.50
Published on Web 04/20/2004

the complex and $[lutH]^+$ is followed by intramolecular proton transfer.

Recently,[3] we reported studies on the kinetics of proton transfer from $[lutH]^+$ to the thiolate sulfur of $[Ni(SR)(triphos)]^+$ (R = Ph or Et), as shown in eq 1. Proton transfer from $[lutH]^+$ to these complexes is relatively slow, and for $[Ni(SEt)(triphos)]^+$, initial protonation of the sulfur is followed by an intramolecular reaction, which we have tentatively attributed to the formation of an η^2-EtSH ligand.

$$[Ni(SR)(triphos)]^+ \underset{lut}{\overset{[lutH]^+}{\rightleftharpoons}} [Ni(SHR)(triphos)]^{2+} \rightleftharpoons [Ni(\eta^2\text{-RS-H})(triphos)]^{2+} \quad (1)$$

In this paper, we report further studies on the reaction between $[Ni(SC_6H_5)(triphos)]^+$ and $[lutH]^+$ in MeCN, which reveal that at high concentrations of acid a more complicated rate law becomes evident. This more complicated rate law is consistent with a two-step mechanism involving initial adduct formation between $[lutH]^+$ and the complex, followed by intramolecular proton transfer to produce $[Ni\{S(H)C_6H_5\}(triphos)]^{2+}$. Additional studies on $[Ni(SC_6H_4R\text{-}4)(triphos)]^+$ (R = NO_2, Cl, Me, or MeO) show that the two-step mechanism is entirely general for this class of complex. Because the kinetics allow us to determine the rate constant for the intramolecular proton transfer, we can, for the first time, systematically investigate the characteristics of this previously unexplored reaction type, including how the 4-R-substituent affects the rates of intramolecular proton transfer, together with the activation parameters and isotope effects.

Experimental Section

All preparations and manipulations were routinely performed under an atmosphere of dinitrogen using Schlenk or syringe techniques as appropriate. All solvents were dried and freshly distilled from the appropriate drying agent immediately prior to use.

The thiols $4\text{-}RC_6H_4SH$ (R = NO_2, Cl, Me, or MeO) and lut (lut = 2,6-dimethylpyridine) were purchased from Aldrich and used as received. $NaSC_6H_4R\text{-}4$,[4] $[NiCl(triphos)]BPh_4$,[3] and $[lutH]BPh_4$[5] and $[lutD]BPh_4$ were prepared by the literature methods.

Preparation of $[Ni(SC_6H_4R\text{-}4)(triphos)]BPh_4$ (R = NO_2, Cl, Me, or MeO). The complexes of the series $[Ni(SC_6H_4R\text{-}4)(triphos)]^+$ were all prepared by the same method[3] which is analogous to that described earlier for $[Ni(SC_6H_5)(triphos)]^+$. The complexes were characterized by elemental and spectroscopic analysis (Table 1), and (for R = MeO, Me, or NO_2) by X-ray crystallography. A typical preparation is described below for $[Ni(SC_6H_4Me\text{-}4)(triphos)]BPh_4$.

A slurry of $[NiCl(triphos)]BPh_4$ (0.5 g, 0.53 mmol) in THF (ca. 30 mL) was stirred rapidly while $NaSC_6H_4Me$ (0.37 g, 2.5 mmol) was added. The mixture rapidly turned from a yellow slurry to a red homogeneous solution. After stirring at room temperature for 1 h, the solution was concentrated to ca. 10 mL, and then, an excess of methanol (ca. 60 mL) was added. Red crystals of the product slowly formed. The crystals were removed by filtration, washed with methanol, then diethyl ether, and dried in vacuo. The product was recrystallized from a dichloromethane/methanol mixture. Yield = 0.32 g (58%).

Table 1. Elemental Analysis and Spectroscopic Characteristics of $[Ni(SC_6H_4R\text{-}4)(triphos)]^+$ (R = NO_2, Cl, Me, or MeO)

	elemental analysis/%[a]			NMR spectroscopy	
R	C	H	N	^1H[b,c]	^{31}P[d]
NO_2	71.4	5.7	1.3		109.8 (t, J_{PP} = 41.0 Hz);
	(71.9)	(5.3)	(1.3)		52.4 (d, J_{PP} = 41.0 Hz)
Cl	68.4	5.8			107.7 (t, J_{PP} = 41.6 Hz);
	(68.6)	(5.1)			54.1 (d, J_{PP} = 42.0 Hz)
Me	71.2	5.5		1.91	106.0 (t, J_{PP} = 41.5 Hz);
	(71.0)	(5.5)			53.8 (d, J_{PP} = 41.3 Hz)
MeO	69.8	5.9		3.43	106.3 (t, J_{PP} = 41.5 Hz);
	(70.0)	(5.4)			54.1 (d, J_{PP} = 41.8 Hz)

[a] Calculated values shown in parentheses. [b] Chemical shifts relative to TMS. [c] Peaks due to triphos ligands are present in all spectra at δ 7.0−8.0 (multiplets, Ph groups) and δ 2.2−3.0 (broad, CH_2). In addition, peaks due to $[BPh_4]^-$ are present in all spectra at δ 6.5−6.9 (multiplets, Ph groups). [d] Chemical shifts relative to H_3PO_4.

X-ray Crystallography. All data were collected on a Bruker SMART CCD area diffractometer, using Mo Kα radiation (λ = 0.71073 Å), by the ω-scan method.[6] Crystal data and other experimental information are given in Table 2, with further details in the Supporting Information. Semiempirical absorption corrections were applied in all cases, on the basis of repeated and symmetry-equivalent reflections.[6] The structures were solved by direct methods and refined by full-matrix least-squares on all unique F^2 values.[7] Anisotropic displacement parameters were assigned to all the non-hydrogen atoms. Hydrogen atoms were placed in idealized positions and allowed to ride on their respective parent atoms. The methyl- and nitro-substituted complexes are THF solvates; H atoms were not included on the THF solvent molecules, which show high thermal motion and are probably somewhat disordered. Although the methyl- and methoxy-substituted complexes appear to be isomorphous, the methoxy derivative is unsolvated; there is 2-fold disorder [refined occupancies 0.712:0.288(2)] for the orientation of the thiolate ligands. The largest peaks in final difference syntheses lie close to solvent and disordered atoms, and close to Ni in the benzyl derivative.

Selected bond lengths and angles for the three substituted benzenethiolate complexes are reported in Table 4.

Kinetic Studies. All kinetic studies were performed using an Applied Photophysics SX.18MV stopped-flow spectrophotometer, modified to handle air-sensitive solutions. The temperature was maintained at 25.0 ± 0.1 °C using a Grant LT D6G thermostated recirculating pump.

All solutions were prepared under an atmosphere of dinitrogen and transferred by gastight, all-glass syringes into the stopped-flow spectrophotometer. Solutions of mixtures of lut and $[lutH]BPh_4$ were prepared from freshly prepared stock solutions and used within 1 h.

The kinetics were studied under pseudo-first-order conditions[8] as described in the previous paper.[1] The high acidity of $[lutH]^+$ (pK_a = 15.4 in MeCN)[9,10] makes it impossible to entirely eliminate

(3) Clegg, W.; Henderson, R. A. *Inorg. Chem.* **2002**, *41*, 1128.
(4) Palermo, R. E.; Power, P. P.; Holm, R. H. *Inorg. Chem.* **1982**, *21*, 173.
(5) Grönberg, K. L. C.; Henderson, R. A.; Oglieve, K. E. *J. Chem. Soc., Dalton Trans.* **1998**, 3093.
(6) *SMART* (control), *SAINT* (integration), *GEMINI* (twinning), and *SADABS* (absorption correction) software; Bruker AXS Inc.: Madison, WI, 2001.
(7) Sheldrick, G. M. *SHELXTL* version 6; Bruker AXS Inc.: Madison, WI, 2001.
(8) Espenson, J. H. *Chemical Kinetics and Reaction Mechanisms*; McGraw-Hill: New York, 1981.
(9) Cauquis, G.; Deronzier, A.; Serve, D.; Vieil, E. *J. Electroanal. Chem. Interfacial Electrochem.* **1975**, *60*, 205.

Table 2. Crystal Data and Structure Refinement Parameters for $[Ni(SC_6H_4R\text{-}4)(triphos)]BPh_4$ (R = Me, MeO, or NO_2) and $[Ni(SCH_2C_6H_5)(triphos)]BPh_4$

	$[Ni(SC_6H_4Me\text{-}4)(triphos)]BPh_4\cdot THF$	$[Ni(SC_6H_4OMe\text{-}4)(triphos)]BPh_4$	$[Ni(SC_6H_4NO_2{-}4)(triphos)]BPh_4\cdot THF$	$[Ni(SCH_2C_6H_5)(triphos)]BPh_4$
chemical formula	$C_{69}H_{68}BNiOP_3S$	$C_{65}H_{60}BNiOP_3S$	$C_{68}H_{65}BNNiO_3P_3S$	$C_{65}H_{60}BNiP_3S$
fw	1107.72	1051.62	1138.70	1035.62
cryst syst	triclinic	triclinic	triclinic	triclinic
space group	$P\bar{1}$	$P\bar{1}$	$P\bar{1}$	$P\bar{1}$
T, K	160	160	160	150
a, Å	11.5726(5)	11.5060(6)	13.6285(6)	12.3581(11)
b, Å	14.5465(6)	14.4698(7)	14.2556(6)	14.4506(13)
c, Å	19.0208(8)	19.4916(10)	16.8955(7)	17.4416(15)
α, deg	76.816(2)	74.030(2)	100.676(2)	79.922(1)
β, deg	84.394(2)	84.610(2)	100.032(2)	69.366(1)
γ, deg	68.235(2)	67.813(2)	114.412(2)	66.256(1)
V, Å^3	2895.0(2)	2888.7(3)	2819.6(2)	2666.2(4)
Z	2	2	2	2
reflns measured	24492	24709	24027	19197
unique data, R_{int}	12859, 0.0217	12924, 0.0299	12567, 0.0195	9315, 0.0592
params	686	731	703	640
R [$F^2 > 2\sigma$]	0.0407	0.0565	0.0414	0.0567
R_w (F^2, all data)	0.1099	0.1654	0.1136	0.1590
absolute structure params				
GOF [F^2]	1.036	1.074	1.042	1.022
max, min electron density (e/Å^3)	0.83, −0.66	1.45, −0.40	1.52, −1.36	1.32, −0.82

Table 3. Summary of Elementary Rate Constants and Equilibrium Constants for the Reactions of $[Ni(SC_6H_4R\text{-}4)(triphos)]^+$ with $[lutH]^+$ and lut in MeCN at 25.0 °C

R	K_2^R/dm^3 mol^{-1}	k_3^R/s^{-1}	k_{-3}^R/dm^3 mol^{-1} s^{-1}	$(k_3^R)^H/(k_3^R)^D$
NO_2	>160	7.0	1×10^4	0.39
Cl	>160	0.19	6	0.88
H	200	0.1	4	
Me	>160	0.05	1.5	1.3
MeO	55.5	0.072	2.5	1.2

all protic impurities in CD_3CN, but ^1H NMR spectroscopic studies show that the acid is at least 90% deuterium-labeled.

Results and Discussion

In the preceding paper,[1] kinetic studies on the reactions of $[Ni(SC_6H_4R\text{-}4)_2(dppe)]$ (R = MeO, Me, H, Cl, or NO_2) with $[lutH]^+$ in the presence of lut indicated that the mechanism involved initial formation of a hydrogen-bonded adduct which subsequently undergoes intramolecular proton transfer. However, only with the R = NO_2 derivative do we observe kinetics which allow us to determine the rate of the intramolecular proton transfer within the hydrogen-bonded adduct. In all the other derivatives a simpler rate law is observed. Consequently, we were unable to probe the factors influencing, and characterizing, the rates of intramolecular proton transfer. In the analogous studies on $[Ni(SC_6H_4R\text{-}4)(triphos)]^+$ (R = MeO, Me, H, Cl, or NO_2) with $[lutH]^+$ reported herein, all complexes exhibit kinetics which allow us to determine the rate constants for intramolecular proton transfer and allow us to define the kinetic characteristics of this type of reaction.

Kinetics and Mechanism. Earlier studies[3] indicated that the protonation of $[Ni(SC_6H_5)(triphos)]^+$ by $[lutH]^+$ in MeCN is an equilibrium reaction {eq 2} associated with the simple rate law shown in eq 3, and $k_1^H = 20 \pm 2$ dm^3 mol^{-1} s^{-1}, $k_{-1}^H = 5 \pm 0.7$ dm^3 mol^{-1} s^{-1}. These rate constants for proton transfer are appreciably slower than the diffusion-controlled limit ($k_{diff} = 1 \times 10^{10}$ dm^3 mol^{-1} s^{-1}).[11] The question then arises whether proton transfer to and from sulfur donor atoms on ligands is inherently slow, or if there is something else causing this decrease in rate specifically in this complex. We, and others,[12,13] have studied the protonation reactions of a variety of complexes and clusters containing sulfur-based ligands. In general, proton transfer to the sulfur sites is rapid. Even proton transfer to μ_3-S atoms in Fe−S-based clusters[14] is appreciably faster than observed in these nickel complexes. Consequently, it would appear that protonation of $[Ni(SC_6H_5)(triphos)]^+$ is slow, either because the proton transfer is thermodynamically unfavorable, or because the sterically demanding $[lutH]^+$ has problems getting sufficiently close to the sulfur to transfer the proton.

$$[Ni(SC_6H_5)(triphos)]^+ + [lutH]^+ \underset{k_{-1}^H}{\overset{k_1^H}{\rightleftharpoons}} [Ni\{S(H)C_6H_5\}(triphos)]^{2+} + lut \quad (2)$$

$$\frac{-d[Ni(SC_6H_5)(triphos)^+]}{dt} = \{k_1^H[lutH^+] + k_{-1}^H[lut]\}[Ni(SC_6H_5)(triphos)^+] \quad (3)$$

In general, the rate constant for protonation of nitrogen or oxygen atoms occurs at the diffusion-controlled limit for thermodynamically favorable reactions and is smaller by a factor of $10^{\Delta pK_a}$ for the reverse (thermodynamically unfavorable) reaction.[11] It is to be expected that the protonation of

(10) Izutsu, K. *Acid−Base Dissociation Constants in Dipolar Aprotic Solvents*; Blackwell-Scientific: Oxford, 1990; p 17.

(11) Bell, R. P. *The Proton in Chemistry*, 2nd ed.; Chapman and Hall: London, 1973; Chapter 7.

(12) (a) Wander, S. A.; Reibenspies, J. H.; Kim, J. S.; Darensbourg, M. Y. *Inorg. Chem.* **1994**, *33*, 1421. (b) Allan, C. B.; Davidson, G.; Choudhury, S. B.; Gu, Z. J.; Bose, K.; Day, R. O.; Maroney, M. J. *Inorg. Chem.* **1998**, *37*, 4166.

(13) Henderson, R. A.; Oglieve, K. E. *J. Chem. Soc., Dalton Trans.* **1999**, 3927.

(14) Bell, J.; Dunford, A. J.; Hollis, E.; Henderson, R. A. *Angew. Chem., Int. Ed.* **2003**, *42*, 1149.

Table 4. Summary of Bond Lengths and Bond Angles in $[Ni(SC_6H_4R\text{-}4)(triphos)]^+$ (R = NO_2, H, Me, or MeO)

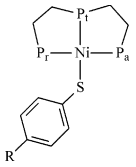

	bond length				bond angle				
R	Ni−P_a	Ni−P_t	Ni−P_r	Ni−S	P_a−Ni−S	P_t−Ni−S	P_r−Ni−S	P_a−Ni−P_r	Ni−S−C
H[a]	2.2101(7)	2.1506(6)	2.1858(7)	2.2456(7)	99.03(3)	173.89(3)	89.76(3)	161.50(3)	99.20(8)
	2.2106(6)	2.1394(6)	2.1987(7)	2.1642(6)	103.99(2)	163.40(3)	89.47(2)	159.79(3)	115.47(8)
NO_2	2.2072(6)	2.1436(6)	2.2406(6)	2.1942(6)	88.38(2)	169.13(2)	102.47(2)	168.57(2)	112.55(7)
Me	2.2066(6)	2.1397(5)	2.2025(5)	2.1685(6)	86.76(2)	163.86(2)	106.68(2)	161.15(2)	121.04(7)
MeO[b]	2.2009(9)	2.1349(8)	2.1986(9)	2.1770(12)	86.88(4)	159.70(5)	107.95(4)	159.41(4)	115.93(17)

[a] Two independent molecules in the asymmetric unit. [b] Major disorder component only.

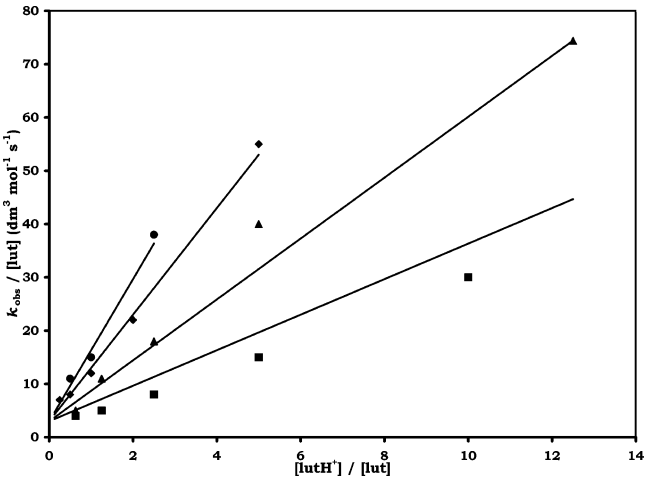

Figure 1. Kinetics for the reaction of $[Ni(SC_6H_5)(triphos)]^+$ with $[lutH]^+$ in the presence of lut (solvent = MeCN) at 25.0 °C. Data points correspond to $[lutH^+]$ = 2.5 mmol dm^{-3}, [lut] = 1−5 mmol dm^{-3} (●); $[lutH^+]$ = 5.0 mmol dm^{-3}, [lut] = 1−20 mmol dm^{-3} (◆); $[lutH^+]$ = 12.5 mmol dm^{-3}, [lut] = 1−20 mmol dm^{-3} (▲); and $[lutH^+]$ = 25.0 mmol dm^{-3}, [lut] = 2.5−40 mmol dm^{-3} (■). Lines drawn are those defined by eq 4.

other atoms containing stereochemical lone pairs of electrons would follow the same reactivity pattern.

The kinetics of the reaction shown in eq 2 have now been studied over a wide concentration range of $[lutH]^+$. Over this extended range, a complicated rate law becomes evident. The kinetic data for the reaction of $[Ni(SC_6H_5)(triphos)]^+$ with $[lutH]^+$ in the presence of lut are shown in Figure 1. The data show that, when $[lutH^+]$ is constant, k_{obs}/[lut] exhibits a linear dependence on the ratio $[lutH^+]$/[lut]. However, at high concentrations of $[lutH]^+$, increasing the concentration of acid leads to a decrease in rate. Analysis of the data shown in Figure 1 results in the rate law shown in eq 4.

$$\frac{-\mathrm{d}[Ni(SC_6H_5)(triphos)^+]}{\mathrm{d}t} = \left\{\frac{20[lutH^+]}{1+200[lutH^+]} + 4[lut]\right\}[Ni(SC_6H_5)(triphos)^+] \quad (4)$$

Equation 4 is consistent with a mechanism[15] involving two coupled equilibria, as illustrated in Figure 2. In this mechanism the initial step in the reaction involves interaction of

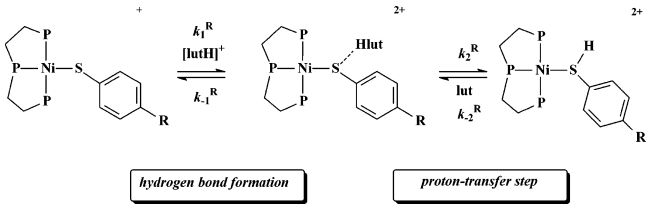

Figure 2. Mechanism for the reaction of $[Ni(SC_6H_4R\text{-}4)(triphos)]^+$ (R = NO_2, Cl, Me. or MeO) with $[lutH]^+$ in the presence of lut (solvent = MeCN), involving initial hydrogen bonding of $[lutH]^+$ to the sulfur followed by proton transfer.

$[lutH]^+$ with $[Ni(SC_6H_5)(triphos)]^+$, but without proton transfer. Subsequent intramolecular proton-transfer produces the coordinated thiol. Since both the nickel complex and the acid are cationic, the initial interaction cannot be electrostatic in origin. It seems more likely that the initial interaction involves hydrogen-bonding, in which the protic end of $[lutH]^+$ hydrogen-bonds to the thiolate sulfur. In addition, this hydrogen-bonding could be augmented by aromatic $\pi-\pi$ stacking[16] of the phenyl groups of the phosphine and the $[lutH]^+$.

Consideration of the mechanism shown in Figure 2 gives the rate law shown in eq 5. The corresponding dependence of k_{obs} on $[lutH^+]$ and [lut] is shown in eq 6, from which eq 7 is readily derived. Equation 7 is the basis of the graph shown in Figure 1. Comparison of eqs 4 and 5 gives the values of the elementary rate constants for the proton-transfer reactions between $[Ni(SC_6H_5)(triphos)]^+$ and $[lutH]^+$ shown in Table 3.

$$\frac{-\mathrm{d}[Ni(SC_6H_4R\text{-}4)(triphos)^+]}{\mathrm{d}t} = \left\{\frac{K_2^R k_3^R [lutH^+]}{1+K_2^R[lutH^+]} + k_{-3}^R[lut]\right\}[Ni(SC_6H_4R\text{-}4)(triphos)^+] \quad (5)$$

$$k_{obs} = \frac{K_2^H k_3^H [lutH^+]}{1+K_2^H[lutH^+]} + k_{-3}^H[lut] \quad (6)$$

Equation 5 describes the full rate law for the mechanism shown in Figure 2. However, when $K_2^R[lutH^+] < 1$, eq 5

(15) Wilkins, R. G. *Kinetics and Mechanism of Reactions of Transition Metal Complexes*; VCH: Weinheim, 1991; pp 33−37.
(16) Martin, N.; Bünzli, J. C.; McKee, V.; Piguet, C.; Hopfgartner, G. *Inorg. Chem*. **1998**, *37*, 577 and references therein.

$$\frac{k_{obs}}{[lut]} = \frac{K_2^{H} k_3^{H} [lutH^+]/[lut]}{1 + K_2^{H}[lutH^+]} + k_{-3}^{H} \quad (7)$$

simplifies to eq 8. Equation 8 is identical in form to that observed in the earlier studies with $[Ni(SC_6H_5)(triphos)]^+$ and $[lutH]^+$ (eq 3) with $k_1^{H} = K_2^{H}k_3^{H}$ and $k_{-1}^{H} = k_{-3}^{H}$. There is good agreement between the values obtained earlier[3] and those observed in this study at the lower concentrations of $[lutH]^+$ (Table 3).

$$k_{obs} = K_2^{H} k_3^{H}[lutH^+] + k_{-3}^{H}[lut] \quad (8)$$

Studies on the reactions of all $[Ni(SC_6H_4R\text{-}4)(triphos)]^+$ (R = NO_2, Cl, Me, or MeO) with $[lutH]^+$ in MeCN show that the kinetics are consistent with the mechanism shown in Figure 2. For R = MeO the observed rate law is analogous to that shown in eq 5. However, for R = Me, Cl, or NO_2, the rate law is simpler.

The kinetics of the reactions between $[Ni(SC_6H_4R\text{-}4)(triphos)]^+$ (R = Me, Cl, or NO_2) and $[lutH]^+$ are similar, but not identical, to those described above for the R = MeO or H analogues. The behavior for the R = Me, Cl, or NO_2 derivatives is typified by the data shown in Figure 3. Thus, at a constant concentration of $[lutH]^+$, $k_{obs}/[lut]$ varies linearly with $[lutH^+]/[lut]$, and increasing the concentration of $[lutH^+]$ decreases the rate. However, under all conditions, varying the concentration of $[lutH]^+$ leads to a linear change in the gradient of the plot of $k_{obs}/[lut]$ against $[lutH^+]/[lut]$. These kinetics are also consistent with the mechanism illustrated in Figure 2, and the rate law shown in eq 5. When $K_2^{R}[lutH^+] > 1$, eq 5 simplifies to eq 9. The graph corresponding to eq 9 is shown in Figure 3 (insert), from which the values of k_3^{R} and k_{-3}^{R} presented in Table 3 were determined.

$$\frac{k_{obs}}{[lut]} = \frac{k_3^{R}}{[lut]} + k_{-3}^{R} \quad (9)$$

Thus, for $[Ni(SC_6H_4R\text{-}4)(triphos)]^+$, when R = MeO or H, the full form of the rate law {eq 5}is observed with the equilibrium constant for the initial binding of the complex and $[lutH]^+$, $K_2^{R} = 55-200$ dm^3 mol^{-1}. For the derivatives where R = Me, Cl, or NO_2, $K_2^{R} > 160$ dm^3 mol^{-1}. Consequently, for R = Me, Cl, or NO_2, under all the experimental conditions we have employed in this study ($[lutH^+] > 12.5$ mmol dm^{-3}), all the nickel complex is bound to $[lutH]^+$. Furthermore, for all the derivatives the slow step in the reaction is the intramolecular transfer of a proton from the $[lutH]^+$ to the sulfur within the hydrogen-bonded adduct. The values of K_2^{R}, k_3^{R}, and k_{-3}^{R} will be considered in a later section, after discussing the structural features of $[Ni(SC_6H_4R\text{-}4)(triphos)]^+$. It is pertinent at this stage to consider why intramolecular proton transfer within a hydrogen-bonded adduct should be slow.

Electronic and Steric Factors Influencing Intramolecular Proton Transfer. There are two possible reasons why the rate of the intramolecular proton transfer in the reactions of $[Ni(SC_6H_4R\text{-}4)(triphos)]^+$ with $[lutH]^+$ is slow. Either the basicity of the thiolate sulfur is very poor or there are steric factors which hold the acid and base sufficiently far apart that the proton transfer is slow because it has to travel a long distance.[17,18] Earlier studies on the reactions between $[Ni(SC_6H_4R\text{-}4)_2(dppe)]$ and $[lutH]^+$ indicate that electronic factors dominate the reactivity. Thus, it is only with the R = NO_2 derivative that intramolecular proton transfer is detected.[1] With complexes containing more electron-releasing substituents, the intramolecular proton transfer cannot be distinguished from the initial formation of the hydrogen-bonded adduct. However, all $[Ni(SC_6H_4R\text{-}4)(triphos)]^+$ derivatives show kinetics in which intramolecular proton transfer within a hydrogen-bonded adduct can be observed. Certainly, it seems reasonable that the sulfur in $[Ni(SC_6H_4R\text{-}4)(triphos)]^+$ would be more electron-poor than in the corresponding $[Ni(SC_6H_4R\text{-}4)_2(dppe)]$ for two reasons. First the complexes are cationic, and second there is a higher proportion of phosphorus coordination. Phosphines are good π-electron-acceptors and so will effectively denude the sulfur of electron density. However, the triphos ligand contains the sterically demanding phenyl substituents which could be a barrier to the approach of the sterically demanding $[lutH]^+$ to the sulfur.

We have determined the X-ray crystal structures of selected $[Ni(SC_6H_4R\text{-}4)(triphos)]^+$ complexes. We have chosen to determine the structures of R = NO_2, Me, and MeO complexes, since these represent 4-R-substituents with markedly different influences and the extremes of electronic effects studied herein. The X-ray crystal structure of $[Ni(SC_6H_5)(triphos)]^+$ was reported by us earlier.[3] Comparison of the structures of $[Ni(SC_6H_4R\text{-}4)(triphos)]^+$ (R = NO_2, Me, or MeO) with that of $[Ni(SC_6H_5)(triphos)]^+$ shows that in all complexes the nickel geometry is best described as distorted square-planar. Figure 4 shows the structure of $[Ni(SC_6H_4NO_2\text{-}4)(triphos)]^+$, which is typical of all the complexes reported herein. While Figure 4 shows the atom numbering scheme for $[Ni(SC_6H_4NO_2\text{-}4)(triphos)]^+$, it is convenient in the following discussion to introduce a more general nomenclature for the phosphorus atoms (illustrated in Figure 5), which focuses on the position of the phosphorus atoms with respect to the lone pairs of electrons on sulfur (the basic site). The two terminal phosphorus atoms are labeled P_r (for the phosphorus remote from the lone pair of electrons on the sulfur) and P_a (for the phosphorus adjacent to the lone pair of electrons on the sulfur), while P_t is the unique secondary phosphorus.

The major bond length and bond angles for $[Ni(SC_6H_4R\text{-}4)(triphos)]^+$ (R = H, NO_2, Me, or MeO) are shown in Table 4. It is evident that there is a significant degree of flexibility in the structural parameters for these complexes. Earlier structural studies[19] on thiolate complexes indicated that a metal−S−C bond angle of ca. 120° was consistent with the coordinated thiolate being under steric strain. In the structures of all $[Ni(SC_6H_4R\text{-}4)(triphos)]^+$ the Ni−S−C angle falls in the range 99−121°. Inspection of the structures of [Ni-

(17) Eigen, M. *Angew. Chem., Int. Ed. Engl.* **1964**, *3*, 1.
(18) Eigen, M. *Z. Phys. Chem. (Frankfurt)* **1954**, *1*, 176.
(19) Orpen, A. G.; Brammer, L.; Allen, F. H.; Kennard, O.; Watson, D. C.; Taylor, R. *J. Chem. Soc., Dalton Trans.* **1989**, 51.

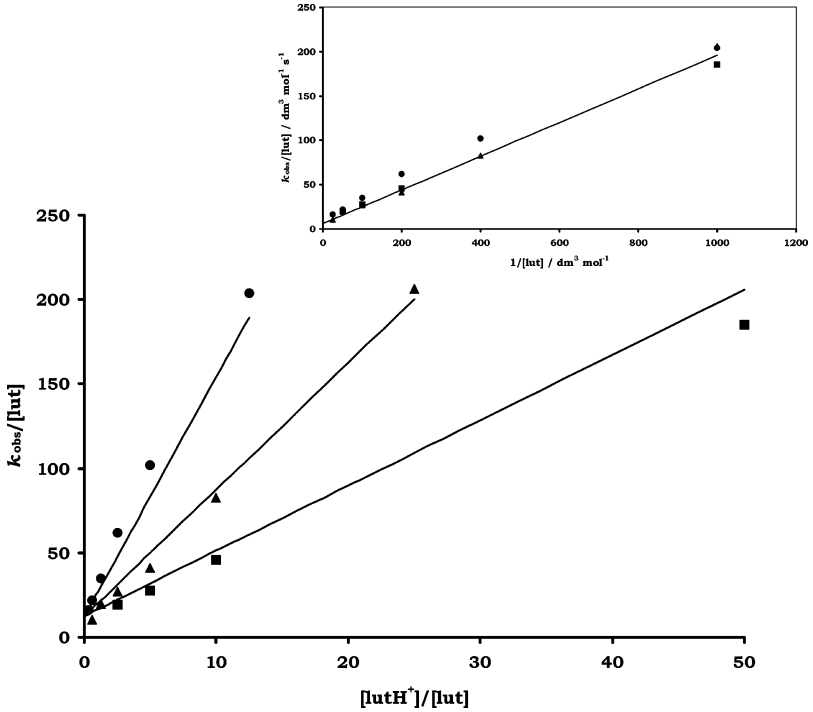

Figure 3. Main: Kinetics for the reaction of $[Ni(SC_6H_4Cl\text{-}4)(triphos)]^+$ with $[lutH]^+$ in the presence of lut (solvent = MeCN) at 25.0 °C. Data points correspond to $[lutH^+] = 12.5$ mmol dm^{-3}, [lut] = 1.0−50.0 mmol dm^{-3} (●); $[lutH^+] = 25.0$ mmol dm^{-3}, [lut] = 1.0−50.0 mmol dm^{-3} (▲); and $[lutH^+] = 50.0$ mmol dm^{-3}, [lut] = 1.0−50.0 mmol dm^{-3} (■). Lines drawn are those defined by eq 7 and the values shown in the text. Insert: The plot of k_{obs}/[lut] against 1/[lut] for the reaction of $[Ni(SC_6H_4Cl\text{-}4)(triphos)]^+$ with $[lutH]^+$ and lut in MeCN at 25.0 °C, using the same data as in the main figure.

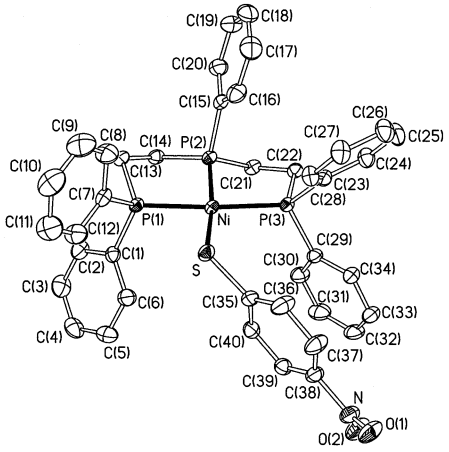

Figure 4. Molecular structure of the cation $[Ni(SC_6H_4NO_2\text{-}4)(triphos)]^+$ showing the atom numbering scheme and 50% probability ellipsoids. H atoms are omitted for clarity.

$(SC_6H_4R\text{-}4)(triphos)]^+$ indicates that the phenyl-groups on P_a and P_t impose significant congestion around the lone-pairs of electrons on sulfur, making the approach of the sterically demanding $[lutH]^+$ to the sulfur site problematical. It seems likely that both electronic and steric factors contribute to making the rate of intramolecular proton transfer slow in $[Ni(SC_6H_4R\text{-}4)(triphos)]^+$ complexes.

As shown in Figure 4, the lone pairs of electrons on sulfur are effectively "buried" in the encapsulating phenyl groups. This becomes particularly important when we consider the trajectory that $[lutH]^+$ must adopt in order to protonate the sulfur. The N−H···S atoms need to be collinear, with the proton approaching one of the lone pairs of electrons. Consideration of the configurations that the coordinated

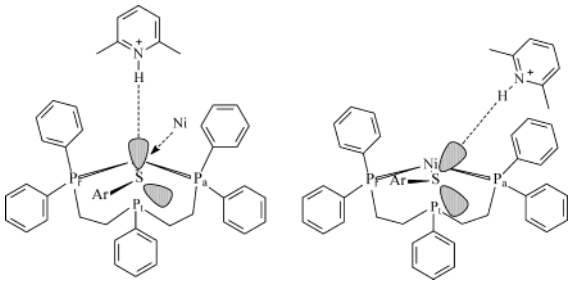

Figure 5. Diagrammatic representation of the limiting geometries showing the orientations of the lone pairs of electrons on the sulfur atom in $[Ni(SC_6H_4R\text{-}4)(triphos)]^+$. In the perspective view drawn on the left-hand side, the nickel atom is "hidden" behind the lone pair.

thiolate can adopt shows there are two limiting orientations of the lone pairs of electrons as shown in Figure 5. It is evident from Figure 5 that approach of $[lutH]^+$ could involve close contact with the phenyl groups on the terminal phosphorus atoms. It seems intuitively reasonable that approach of $[lutH]^+$ should take the line of least interaction, which is perpendicular to the square-planar complex. Approach of $[lutH]^+$ from above the $NiSP_3$ plane is only possible if (i) there is rotation of the thiolate around the Ni−S bond so that one of the lone pairs of electrons is pointing directly in the correct orientation and (ii) the lone pair of electrons on sulfur and the phenyl group on P_t are on opposite sides of the plane. This optimized orientation is shown on the left-hand side of Figure 5. Even if these conditions are satisfied, the approach of the sterically demanding $[lutH]^+$ to the sulfur is difficult. The result is that proton transfer from $[lutH]^+$ to sulfur in $[Ni(SC_6H_4R\text{-}4)(triphos)]^+$ is likely to have to occur over an appreciable distance to a poorly basic sulfur, resulting in slow intramolecular proton transfer reaction.

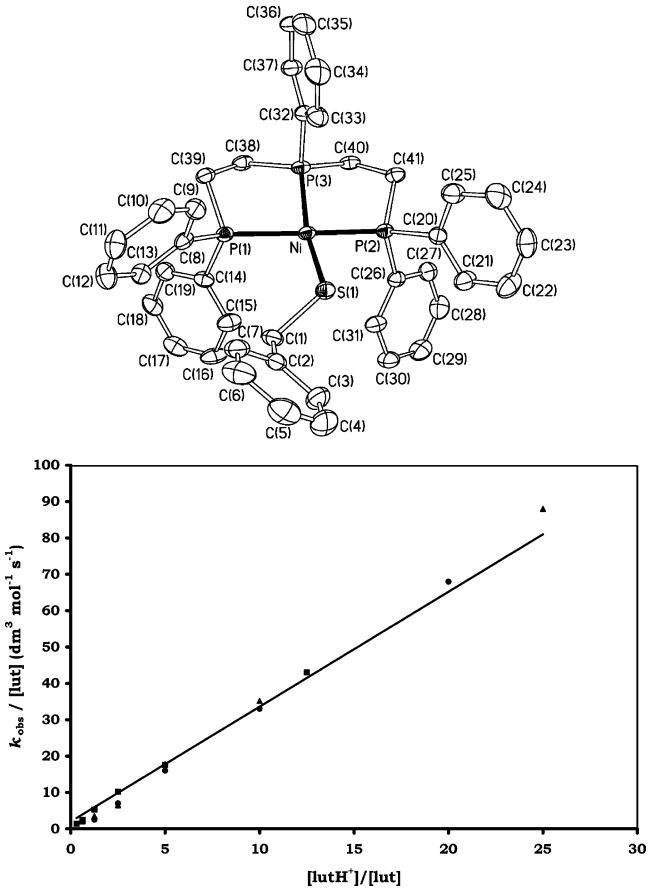

Figure 6. Top: Molecular structure of $[Ni(SCH_2C_6H_5)(triphos)]^+$ with 50% probability displacement ellipsoids and without H atoms. Selected dimensions and angles are Ni−P(1) = 2.2042(10) Å; Ni−P(2) = 2.1960(10) Å; Ni−P(3) = 2.1468(10) Å; Ni−S = 2.1689(10) Å; P(1)−Ni−P(2) = 161.90(4)°; P(1)−Ni−S = 103.95(4)°; P(2)−Ni−S = 89.66(4)°; P(3)−Ni−S = 164.01(4)°; Ni−S−C(1) = 115.18(13)°. Bottom: Kinetic data for the reaction of $[Ni(SCH_2C_6H_5)(triphos)]^+$ with $[lutH]^+$ in the presence of lut in MeCN at 25.0°. Data points correspond to $[lutH^+]$ = 12.5 mmol dm^{-3}, [lut] = 1.0−40.0 mmol dm^{-3} (■); $[lutH^+]$ = 25.0 mmol dm^{-3}, [lut] = 1.0−40.0 mmol dm^{-3} (▲); $[lutH^+]$ = 50.0 mmol dm^{-3}, [lut] = 2.5−40.0 mmol dm^{-3} (●).

The discussion presented above indicates that in the $[Ni(SC_6H_4R\text{-}4)(triphos)]^+$ system both electronic and steric factors could contribute to slow intramolecular proton transfer rates. However, studies on the reaction between $[lutH]^+$ and $[Ni(SCH_2C_6H_5)(triphos)]^+$ indicate that electronic factors dominate in controlling the rate of intramolecular proton transfer.

The reaction between $[Ni(SCH_2C_6H_5)(triphos)]^+$ and mixtures of $[lutH]^+$ and lut exhibit simple kinetics as shown in Figure 6 (bottom) and described by eq 10.

$$\frac{-d[Ni(SCH_2C_6H_5)(triphos)^+]}{dt} = \{3.2[lutH^+] + 2.0[lut]\}[Ni(SCH_2C_6H_5)(triphos)^+] \quad (10)$$

Equation 10 is consistent with the simple, single step equilibrium reaction shown in eq 11, with k_1^{Bn} = 3.2 dm^3 mol^{-1} s^{-1} and k_{-1}^{Bn} = 2.0 dm^3 mol^{-1} s^{-1} (the superscript Bn denotes benzyl). It is reasonable to assume that the k_1^{Bn} step comprises initial adduct formation (K_2^{Bn}) followed by proton transfer (k_3^{Bn}). If adduct formation were kinetically distinguishable from proton transfer then the kinetics would follow the rate law shown in eq 5. Since the kinetic data for the reaction of $[Ni(SCH_2C_6H_5)(triphos)]^+$ with $[lutH]^+$ show no evidence for departure from the simple kinetics defined by eq 11, even at the highest concentration of $[lutH]^+$ used ($[lutH^+]$ = 50 mmol dm^{-3}), we can establish from eq 5 that $K_2^{Bn}[lutH^+] \leq 0.1$, and that $K_2 \geq 2$ dm^3 mol^{-1}.

$$[Ni(SCH_2C_6H_5)(triphos)]^+ + [lutH]^+ \underset{k_{-1}^{Bn}}{\overset{k_1^{Bn}}{\rightleftharpoons}} [Ni\{S(H)CH_2C_6H_5\}(triphos)]^{2+} + lut \quad (11)$$

The X-ray crystal structure of $[Ni(SCH_2C_6H_5)(triphos)]BPh_4$ is shown in Figure 6 (top), and the bond lengths and bond angles for this cation, which are decribed in the legend, are very similar to those of $[Ni(SC_6H_4R\text{-}4)(triphos)]^+$. It is particularly noteworthy that the dimensions associated with the $\{Ni(triphos)\}^{2+}$ core in the benzyl-derivative is extremely similar to that in the aryl-derivatives. It is the disposition of the phenyl-groups on the triphos ligand which represent the most important barrier to approach of the $[lutH]^+$. Thus, the difference in the kinetics is most reasonably attributable to the difference in the basicities of the sulfur sites in the benzyl- and aryl-thiolates. It would be anticipated that the alkanethiolate ligand would be more basic than the aryl thiolate ligand. If steric factors dominated the rates of proton transfer to sulfur in these complexes, then the benzyl and aryl derivatives would show similar kinetics.

Isotope Effects. The isotope effects for the reactions between $[Ni(SC_6H_4R\text{-}4)(triphos)]^+$ (R = NO_2, Cl, or MeO) and $[lutD]^+$ have been determined, allowing us to investigate the effect of changing the basicity of the sulfur site on the kinetic isotope effect associated with proton transfer. In order to ensure that, for all complexes, we were measuring the kinetic isotope effect associated with the elementary reaction of intramolecular proton transfer, all experiments were performed with $[lutH^+]$ > 25 mmol dm^{-3} so that all the nickel complex is hydrogen-bonded to $[lutH^+]$.

The kinetic isotope effect for k_3^R varies with the 4-R-substituent. The results of the experiments with $[lutD]^+$ are illustrated in Figure 7 and are summarized for all the complexes in Table 3.

Inspection of the results in Table 3 shows that, in general, complexes containing the most electron-withdrawing 4-R-substituent (R = NO_2) exhibit an inverse kinetic isotope effect, $(k_3^{NO_2})^H/(k_3^{NO_2})^D$ = 0.39, but as R becomes more electron-releasing there is a change so that when R = Me or MeO a primary kinetic isotope effect is observed, $(k_3^{Me})^H/(k_3^{Me})^D$ = 1.3, $(k_3^{MeO})^H/(k_3^{MeO})^D$ = 1.2. With $[Ni(SC_6H_4Cl\text{-}4)(triphos)]^+$, where the 4-R-substituent has an electronic effect intermediate between those of MeO and NO_2, we observe an intemediate kinetic isotope effect, $(k_3^{Cl})^H/(k_3^{Cl})^D$ = 0.88.

The isotope effects associated with the reverse reaction (k_{-3}^R) are not easy to measure. The error in the intercepts of the graphs typified by those shown in Figure 6 means that it is difficult to confidently determine $(k_{-3}^R)^H/(k_{-3}^R)^D$ ac-

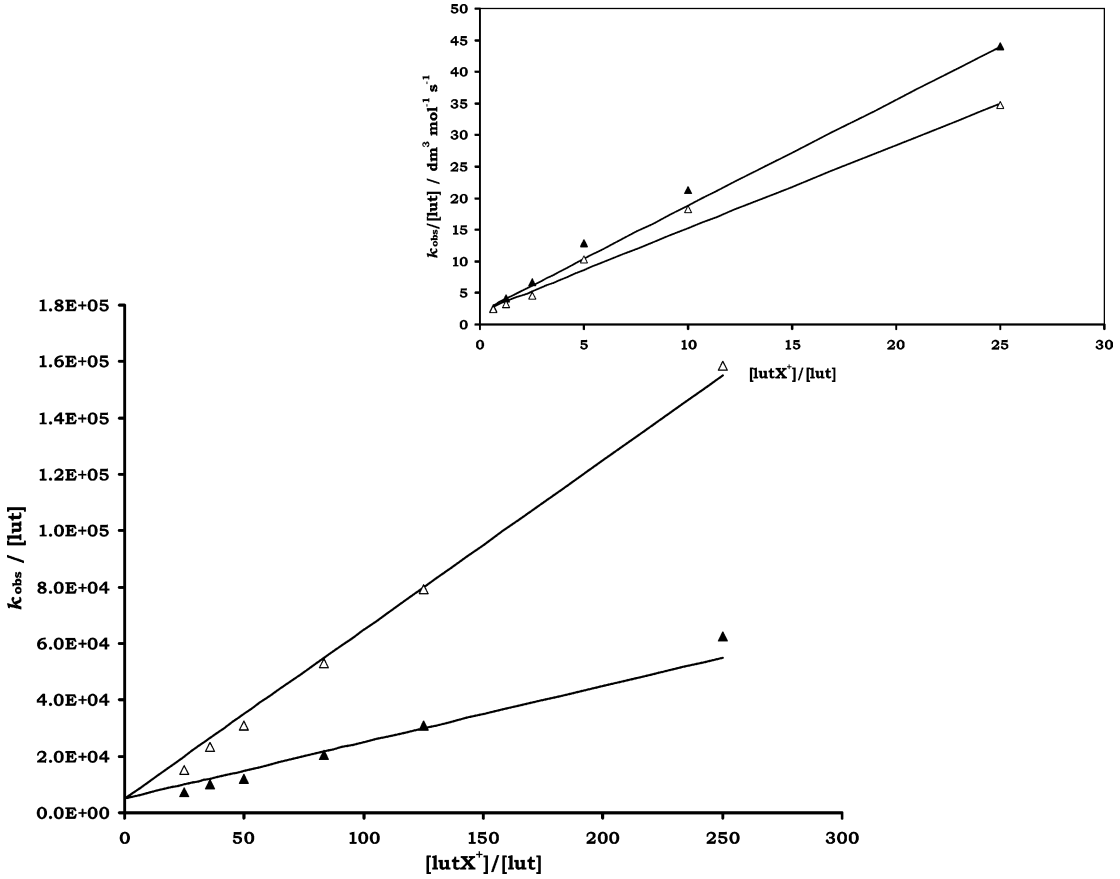

Figure 7. Kinetic data showing the isotope effects for the reactions between $[Ni(SC_6H_4R\text{-}4)(triphos)]^+$ and $[lutX]^+$ (X = H or D) in the presence of lut (solvent = MeCN) at 25.0 °C. Main: R = NO_2; $[lutH^+]$ = 25.0 mmol dm^{-3}, [lut] = 0.1−1.0 mmol dm^{-3} (▲), studies with $[lutD]^+$ are shown as open symbols. Insert: R = MeO; $[lutH^+]$ = 25.0 mmol dm^{-3}, [lut] = 1.0−40.0 mmol dm^{-3} (▲), studies with $[lutD]^+$ are shown as open symbols.

curately. However, inspection of the graphs indicates that the kinetic isotope effect associated with k_{-3}^R is smaller than that for k_3^R.

A simplistic picture of the intramolecular proton transfer step being monitored in these experiments involves $[lutH]^+$ hydrogen-bonding to the sulfur. The position of the proton within the hydrogen-bonded adduct, and the transition state for proton transfer, is influenced only by the basicity of the sulfur which is modulated by the 4-R-substituent. The steric constraints imposed by the phenyl groups of the triphos are reasonably assumed to be essentially the same for all $[Ni(SC_6H_4R\text{-}4)(triphos)]^+$. It seems likely that, with the most electron-releasing 4-R-substituent (MeO), in the ground state, the proton is closest to the sulfur and furthest from the nitrogen. At the other extreme, with the most electron-withdrawing 4-R-substituent (NO_2), the proton is still predominantly associated with the lut residue. It seems reasonable that there is a spectrum of such configurations, with the position of the proton in the ground state varying with the electronic influence of the 4-R-substituent.

Using the intuitive picture described above, together with the experimental observations, it appears that intramolecular transfer of a proton to the least basic sulfur sites is associated with an inverse primary isotope effect. The apparent correlation of $(k_3^R)^H/(k_3^R)^D$ with the 4-R-substituent indicates that as the sulfur site becomes more basic, the kinetic isotope effect becomes larger.

It is unexpected that the intramolecular proton transfer reactions are associated with a variety of kinetic isotope effects. Previous theoretical and experimental studies[20−22] have indicated that kinetic deuterium isotope effects may become inverse when (i) the product has a very strong vibrational force constant compared to the reactant, and the transition state is product-like, or (ii) a stepwise sequence involving transfer of the proton (to an atom with which it vibrates at a higher frequency) occurs prior to the rate-limiting step. Our results indicate that, in intramolecular proton transfer reactions within a hydrogen-bonded adduct, an inverse kinetic isotope effect is observed when the base is relatively weak and the transition state is reactant-like, while a normal kinetic isotope effect is observed with stronger bases, and the transition state is product-like.

Temperature Effects. We have investigated the effect of temperature on the rate of the reaction between $[lutH]^+$ and $[Ni(SC_6H_4R\text{-}4)(triphos)]^+$ and, hence, determined the activation parameters ($\Delta H^‡$ and $\Delta S^‡$) for the intramolecular proton transfer.

Eyring plots comparing the temperature dependences of the reactions of $[lutH]^+$ with $[Ni(SC_6H_4Cl\text{-}4)(triphos)]^+$, $[Ni(SC_6H_4NO_2\text{-}4)(triphos)]^+$, and $[Ni(SC_6H_4OMe\text{-}4)(triphos)]^+$ are shown in Figure 8, and the values of $\Delta H^‡$ and $\Delta S^‡$ are

(20) Parkin, G.; Bercaw, J. E. *Organometallics* **1989**, *8*, 1172.
(21) Bigeleisen, *J. Pure Appl. Chem.* **1964**, *8*, 217.
(22) Melander, L. *Acta Chem. Scand.* **1971**, *25*, 3821.

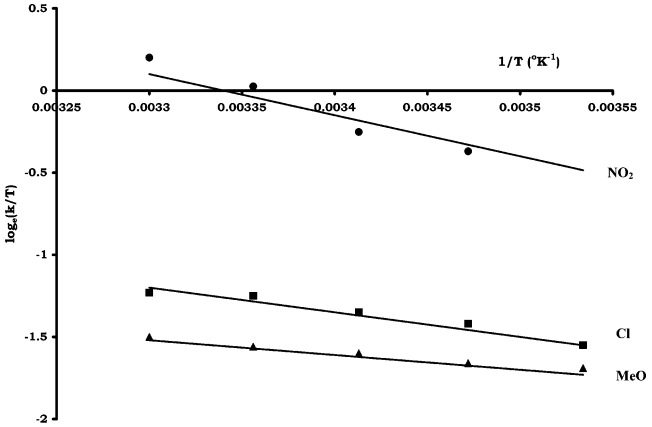

Figure 8. Eyring plots for the temperature dependences of the reactions between $[Ni(SC_6H_4R\text{-}4)(triphos)]^+$ {R = NO_2 (●), Cl (■), or MeO (▲)} and $[lutH]^+$ in the presence of lut (solvent = MeCN).

Table 5. Activation Parameters for the Intramolecular Proton Transfer Reaction between $[Ni(SC_6H_4R\text{-}4)(triphos)]^+$ and $[lutH]^+$

complex	$\Delta H^{\ddagger}$/ kcal mol^{-1}	$\Delta S^{\ddagger}$/ cal K^{-1} mol^{-1}	$\Delta G^{\ddagger}_{298}$/ kcal mol^{-1}	k_3/s^{-1} (at 25.0 °C)
$[Ni(SC_6H_4OMe)(triphos)]^+$	4.1	−50.1	19.0	0.07
$[Ni(SC_6H_4Me\text{-}4)(triphos)]^+$	6.9	−41.2	19.2	0.05
$[Ni(SC_6H_4NO_2{-}4)(triphos)]^+$	11.4	−16.4	16.3	7.0

summarized in Table 5. There is a clear systematic trend which parallels both the isotope effects observed with the same compounds, and the trend observed in the protonation reactions of $[Ni(SC_6H_4R\text{-}4)_2(dppe)]$ in the previous paper.[1]

As the 4-R-substituent becomes more electron-withdrawing, $\Delta H^{\ddagger}$ increases and $\Delta S^{\ddagger}$ becomes less negative. The marked variation in the values of $\Delta H^{\ddagger}$ and $\Delta S^{\ddagger}$ observed with different 4-R-substituents deserves further comment. For all complexes $\Delta H^{\ddagger}$ is small, while the corresponding values of $\Delta S^{\ddagger}$ are negative. Both parameters show a marked dependence on the 4-R-substituents.

The magnitude of $\Delta H^{\ddagger}$ reflects the relatively large distance that the proton has to move. That $\Delta H^{\ddagger}$ is largest and $\Delta S^{\ddagger}$ least negative for complexes containing electron-withdrawing 4-R-substituents is consistent with the description presented above in which the nitrogen−proton−sulfur configuration in the hydrogen-bonded adduct depends on the electronic influence of the 4-R-substituent. The reactions of complexes with electron-releasing 4-R-substituents are associated with the smallest $\Delta H^{\ddagger}$ since the thiolate is the most basic, and in the ground state the proton is closer to the sulfur.

It is worth noting that $\Delta S^{\ddagger}$ is most negative in the reactions of complexes containing electron-releasing 4-R-substituents on the thiolate and becomes more positive as the 4-R-substituent becomes more electron-withdrawing. This behavior indicates that in the reactions involving electron-releasing 4-R-substituents the transition state is more product-like (i.e., the proton is more transferred to the sulfur). Simplistically, the negative $\Delta S^{\ddagger}$ in the reactions involving complexes containing electron-releasing substituents is rationalizable, since the transition state for the proton transfer in these systems involves the proton closer to the sulfur. Consequently, the lut residue is only weakly bound to the complex and thus has more degrees of freedom.

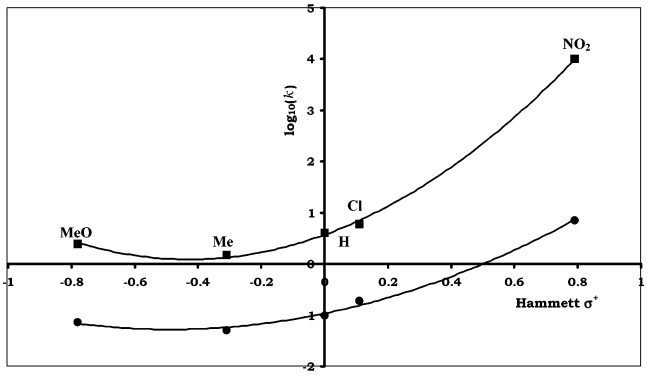

Figure 9. Hammett plots for the reaction of $[Ni(SC_6H_4R\text{-}4)(triphos)]^+$ (R = NO_2, Cl, H, Me, or MeO) with $[lutH]^+$ in the presence of lut (solvent = MeCN) at 25.0 °C. The data points correspond to k_3^R (●) and k_{-3}^R (■). The curves are only trendlines and do not represent a mathematical fit to the data.

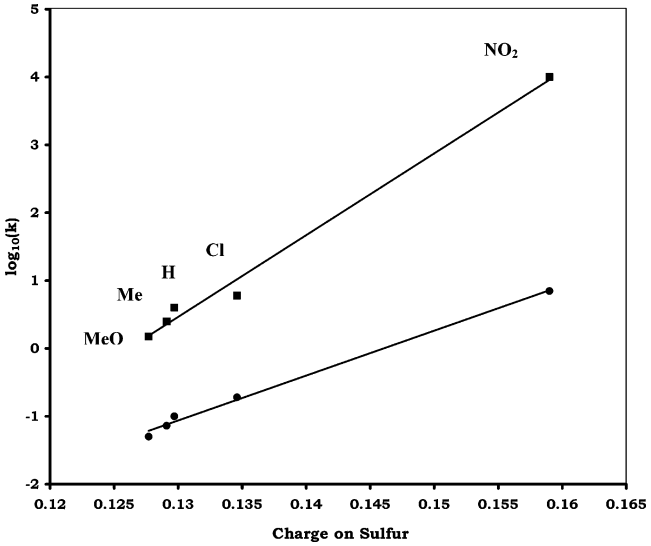

Figure 10. Graph showing the linear variation of $\log(k_3)$ (●) and $\log(k_{-3})$ (■) against the charge on the sulfur atom calculated using the Normal Bond Order method.

Electronic Effects of 4-R−Substituents on Thiolate. A semiquantitative measure of how 4-R-substituents on the coordinated thiolate influence the rate of intramolecular proton transfer is the Hammett plot shown in Figure 9. An interesting feature of the rates of intramolecular proton transfer described in this paper is that electron-withdrawing 4-R-substituents facilitate intramolecular proton transfer, while electron-releasing 4-R-substituents have a less marked influence on the rate.

Figure 9 shows a markedly nonlinear dependence of $\log(k_3^R)$ on Hammett σ^+. We have chosen to use the Hammett σ^+ since these parameters[23] allow for the conjugation between the 4-R-substituent and the rest of the molecule; this seems to be particularly important for ligands coordinated to transition metal sites.[24]

Basu et al.[25] have recently pointed out that the Hammett σ^+ parameter only describes resonance effects and neglects

(23) Alder, R. W.; Baker, R.; Brown, J. M. *Mechanism in Organic Chemistry*; Wiley: London, England, 1971; pp 28−39.
(24) Hussain, W.; Leigh, G. J.; Mohd Ali, H.; Pickett, C. J.; Rankin, D. A. *J. Chem. Soc., Dalton Trans.* **1984**, 1703.
(25) Sengar, R. S.; Nemykin, V. N.; Basu, P. *New J. Chem.* **2003**, *7*, 1115.

inductive effects. Theoretical calculations indicate that the HOMO in thiols and disulfides is delocalized between the π-orbital of the benzene ring and the p_z-orbital on the sulfur. Electron-donating 4-R-substituents destabilize the energy of the HOMO, and electron-releasing 4-R-substituents stabilize the HOMO.[26,27]

The charge on the sulfur atom with various 4-RC_6H_4S- derivatives has been calculated[25] using the Natural Bond Order package. We have used these calculated charges and (as shown in Figure 10) shown that this correlates well with the rates of intramolecular proton transfer. This correlation indicates that it is the electron density on the sulfur which controls the rate of proton transfer within the hydrogen-bonded adduct.

Summary

The studies on $[Ni(SC_6H_4R\text{-}4)(triphos)]^+$ described in this paper, together with the results on $[Ni(SC_6H_4R\text{-}4)_2(dppe)]$ reported in the preceding paper,[1] indicate that the mechanism for transfer of a proton from $[lutH]^+$ to sulfur in these complexes involves a two-step mechanism, in which an initial hydrogen bonding interaction between the acid and complex is followed by an intramolecular proton transfer reaction. There is nothing unusual about this mechanism. Indeed, all proton transfer reactions must involve this type of two-step process. However, rarely is the initial binding of the acid to the base distinguishable from the transfer of the proton. In the majority of proton transfer reactions there is no appreciable steric barrier to the acid−base pair getting sufficiently close to result in rapid transfer of the proton. The reason we can observe the hydrogen-bonding as a prequel to proton transfer in this case is (i) because the base (sulfur) is buried in the complex surrounded by bulky phenyl rings, and the acid ($[lutH]^+$) is sterically demanding and is held an appreciable distance from the sulfur, so that proton transfer has to occur across some distance and is consequently slow, and (ii) because the aryl thiolate sulfur is poorly basic. In the reactions of $[Ni(SC_6H_4R\text{-}4)(triphos)]^+$ with $[lutH]^+$ the acid must not only migrate to the solvation shell of the complex but also penetrate the array of phenyl groups which surround the sulfur atom. Because intramolecular proton transfer within the hydrogen-bonded adduct is rate-limiting in the reactions of $[Ni(SC_6H_4R\text{-}4)(triphos)]^+$ with $[lutH]^+$, we have been able to study how systematic electronic changes to the basicity of the sulfur affect the rates, activation parameters ($\Delta H^{\ddagger}$ and $\Delta S^{\ddagger}$), and kinetic isotope effects of this elementary reaction.

Supporting Information Available: X-ray crystallographic files in CIF format for the crystal structures and kinetic data for the reactions of $[Ni(SC_6H_4R\text{-}4)(triphos)]$ (R = MeO, Me, H, Cl, or NO_2). This material is available free of charge via the Internet at http://pubs.acs.org.

IC0303237

(26) McGuire, D. G.; Khan, M. A.; Ashby, M. T. *Inorg. Chem.* **2002**, *41*, 2202.
(27) Sellmann, D.; Sutter, J. *Acc. Chem. Res.* **1997**, *30*, 460.